



Temperature dependence of the short-range order of Cu₆₅Zr₃₅ metallic glass

N. Mattern^{a,*}, J. Bednarcik^b, M. Stoica^a, J. Eckert^{a,c}

^a IFW Dresden, Institute for Complex Materials, Helmholtzstr. 20, D-01069 Dresden, Germany

^b Hasylab at DESY, Notkestr. 85, D-22603 Hamburg, Germany

^c TU Dresden, Institute of Materials Science, Helmholtzstr. 7, D-01062 Dresden, Germany

ARTICLE INFO

Article history:

Received 1 June 2012

Received in revised form

19 July 2012

Accepted 16 August 2012

Available online xxx

Keywords:

B. Glasses, metallic

B. Thermal properties

F. Diffraction

ABSTRACT

The thermal behaviour of the short-range order of Cu₆₅Zr₃₅ metallic glass has been investigated by means of in situ high energy synchrotron X-ray diffraction. The temperature dependence of the X-ray structure factor and the atomic pair correlation function was analysed within the glassy state. In addition to the effect of volume expansion and thermal atomic oscillations changes occur in the short-range order. Local atomic rearrangements take place as a consequence of the structural heterogeneity in the glass. The structural transformations depend linearly on temperature. The changes of the short-range order of the glass by thermal expansion are found to be different from those under elastic tensile strain.

© 2012 Elsevier Ltd. All rights reserved.

1. Introduction

Bulk metallic glasses (BMGs) exhibit excellent mechanical properties like a high strength at almost the theoretical limit, a large elasticity range up to 2% and a lower Young's modulus compared to their crystalline counterparts [1–4]. Much effort has been devoted in the last years to improve the glass-forming ability and to analyse the physical properties of BMGs in order to use them in different applications [5]. Most BMGs are multi-component alloys with a number of elements $n \geq 3$, which does not allow to extract element-specific structure information from diffraction data due to superposition of the $n(n+1)/2$ partial atomic pair correlations. Moreover, the possibilities of structure simulations are strongly restricted for multi-component alloys. Thus, binary metallic liquids and glasses are the most suitable systems for experimental investigations and for modelling the atomic structure. The reports on successful preparation of bulk glasses by casting of binary Cu–Zr alloys [6–8] promoted several theoretical and experimental structure investigations in the last years [9–19]. Our current understanding of the structure on the atomic scale is mainly based on molecular dynamics (MD) simulations of binary melts upon quenching. The local structure of Cu–Zr glasses prepared by MD was found to consist of a variety of densely packed polyhedral arrangements with high coordination numbers [9–12]. Quite similar polyhedra are found also by Reverse Monte Carlo models at room temperature using experimental diffraction data of Cu–Zr glasses

[16,17]. The relative fraction of the different coordination polyhedra among icosahedra as a dominant motive varies with composition and quenching rate, respectively [10]. The latter relates to temperature dependent structural changes occurring to the largest extent through the liquid–glass transition. As a consequence of the structural changes, the parameters position and height of the first diffuse maximum of the structure factor of Cu–Zr liquids show a strong dependence on composition and temperature in the simulations which are found to be in accordance with experimental data [13]. Sudden changes of the short-range order upon cooling of liquid Cu₄₆Zr₅₄ were reported recently which were attributed to a rapid development of chemically ordered icosahedral clusters [19].

The aim of this work was to analyse the temperature dependence of the short-range order of Cu₆₅Zr₃₅ in the glassy state. The results of in situ X-ray diffraction measurements will show that beside thermal expansion, the atomic structure of the glass changes with temperature.

2. Experimental

Rapidly quenched glassy ribbons which were prepared from a Cu₆₅Zr₃₅ prealloy by single roller melt-spinning under Ar atmosphere. The resulting ribbons had a width of about 4 mm and thickness of about 35 μm. Rods of 1 mm were obtained by suction casting into a copper mould. The thermal behaviour of the as-cast ribbon was investigated by differential scanning calorimetry (DSC) under argon employing a Netzsch DSC 404 calorimeter (heating rate 10 K/min). In situ X-ray diffraction (XRD) at elevated temperatures

* Corresponding author. Tel.: +49 3514659367.

E-mail address: n.mattern@ifw-dresden.de (N. Mattern).

was performed at the high-energy synchrotron beam line BW5 (HASYLAB at DESY Hamburg) at 100.0 keV photon energy corresponding to a wave-length of 0.01249 nm. Pieces of $\text{Cu}_{65}\text{Zr}_{35}$ glassy ribbons with an average size of about 100 μm were filled into 2 mm glass capillaries. The samples were heat treated in a computer controlled Linkam hot stage (the heating rate was 10 K/min). First, for relaxation the temperature was increased from room temperature up to 673 K, then decreased to 330 K. Then the samples were heated up again from 330 K to 773 K. The XRD patterns were recorded simultaneously by a 2-dimensional detector (Perkin Elmer PE1621) for every 3 K (the acquisition time was 20 s). The distance between sample and detector was 280 mm. For data analysis the Fit2D program was used [20]. The linear thermal expansion coefficient was determined by a Netzsch DIL 402 C dilatometer under argon atmosphere at a heating rate of 5 K/min. The mass density at room temperature was estimated by the buoyancy method from the weight difference in air and in dodecane ($\text{C}_{12}\text{H}_{26}$).

3. Experimental results

3.1. Thermal behaviour

The thermal behaviour of the amorphous $\text{Cu}_{65}\text{Zr}_{35}$ alloy is shown in Fig. 1 by its DSC trace recorded upon constant-rate heating at 20 K/min. The glass transition at $T_g = 750$ K and the crystallization at $T_x = 773$ K observable by the respective endothermic and exothermic heat flow events are in good agreement with values reported in literature [15]. Fig. 2 shows the relative length change $\Delta L/L_0$ of the glassy $\text{Cu}_{65}\text{Zr}_{35}$ rod versus temperature measured upon heating. A thermal expansion coefficient $\alpha = 10.4 \cdot 10^{-6}/\text{K}$ is obtained by a linear fit of the data between 400 and 700 K. The glass transition is not visible in the dilatometer measurement possibly due to the lower crystallization temperature for the applied heating rate of 5 K/min. The density increase associated with the crystallization is reflected by the shrinkage of the sample.

3.2. Analysis of reciprocal space diffraction data

In order to avoid errors by contributions of relaxation and beginning crystallization the analysed diffraction data discussed in

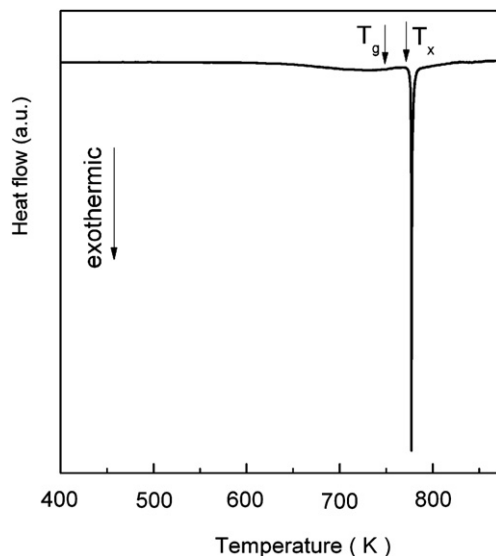


Fig. 1. DSC scan of $\text{Cu}_{65}\text{Zr}_{35}$ glass at 20 K/min heating rate, the glass transition temperature T_g and the crystallization temperature T_x are marked by arrows.

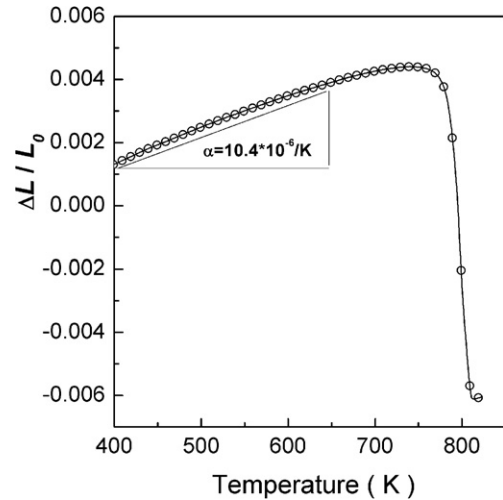


Fig. 2. Thermal expansion $\Delta L/L_0$ of $\text{Cu}_{65}\text{Zr}_{35}$ BMG at 5 K/min heating rate.

the following were restricted to the second heating cycle and the temperature range between 330 and 700 K in the following.

Fig. 3 shows the structure factor $S(q)_T$ of the alloy from room temperature up to elevated temperatures. The structure factor $S(q)$ was calculated from the measured intensities after radial integration of the data and applying the usual corrections and normalization procedure to determine the coherent scattered intensity in absolute electron units [21]:

$$S(q) = \frac{I_{e.u.}^{\text{coh}} - (\langle f^2 \rangle - \langle f \rangle^2)}{\langle f \rangle^2} \quad (1)$$

with $\langle f \rangle^2 = (\sum c_i f_i)^2$ and $\langle f^2 \rangle = \sum c_i \cdot f_i^2$, where f_i is the atom form amplitude of the element i and c_i is the concentration. The amorphous structure is preserved up to the highest temperature of 700 K. The structure factors exhibit small changes of the positions

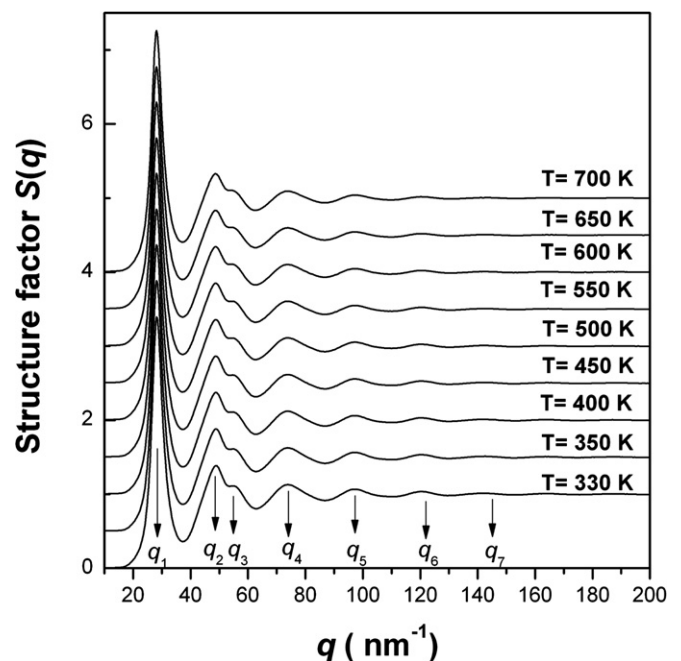


Fig. 3. Structure factor $S(q)$ of $\text{Cu}_{65}\text{Zr}_{35}$ glass at different temperatures.

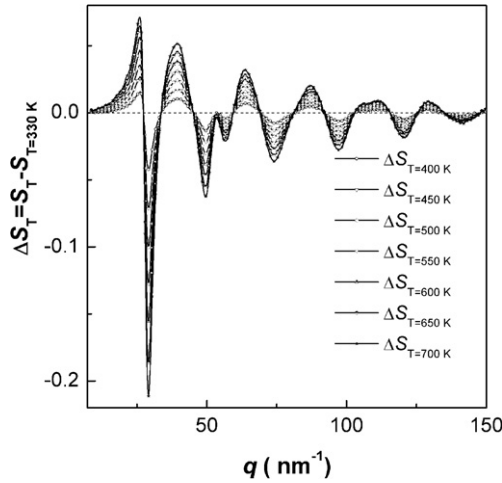


Fig. 4. Difference curves between the structure factor $\Delta S(q)_T = S(q)_T - S(q)_{T=330 \text{ K}}$ at room temperature and elevated temperatures.

and heights of the maxima with increasing temperature. Besides a shift in the positions of the maxima, the oscillations of the structure factor around the value $S(q) = 1$ become reduced, i.e. the intensities of the maxima decrease, and those of the minima increase. The changes of the structure factor with temperature are shown in Fig. 4 by the corresponding difference curves $\Delta S(q)_T = S(q)_T - S(q)_{T=330 \text{ K}}$ between the measurement at different temperatures T and room temperature, respectively. The observed changes of $S(q)_T$ within the glassy state exhibit a linear dependence with T , which means that $\Delta S(q)_T/\Delta T$ does not depend on the temperature (at least within the error limits).

Fig. 5 shows the thermal behaviour of the position of the first maximum q_1 and its height $S(q_1)$, respectively. Both quantities decrease with temperature. From a linear fit of the experimental data a linear thermal coefficient $(1/q_1) \cdot \delta q_1(T)/\delta T = 12.5 \cdot 10^{-6}/\text{K}$ is calculated, which approximately corresponds to the macroscopic thermal expansion coefficient as determined by the dilatometer measurements.

The influence of temperature on $S(q)$ can be calculated for two ideal cases: volume expansion by increase of all inter-atomic distances, and enhancement of harmonic oscillations of the atoms with temperature. Assuming that the volume expansion does not alter the relative arrangements of the atoms, the length scales from r to $r(1 + \epsilon)$, the change $\Delta S(q)_T$ is given by:

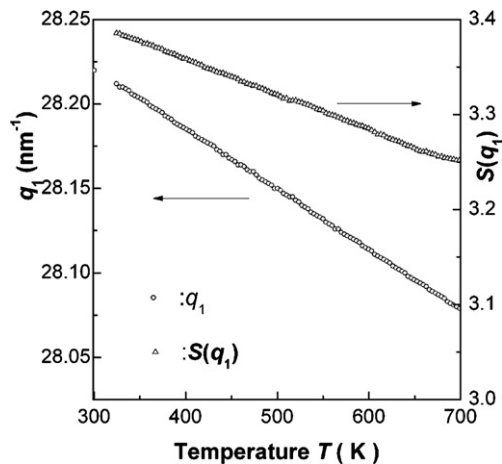


Fig. 5. Position and height of the first maximum of $S(q)$ versus temperature.

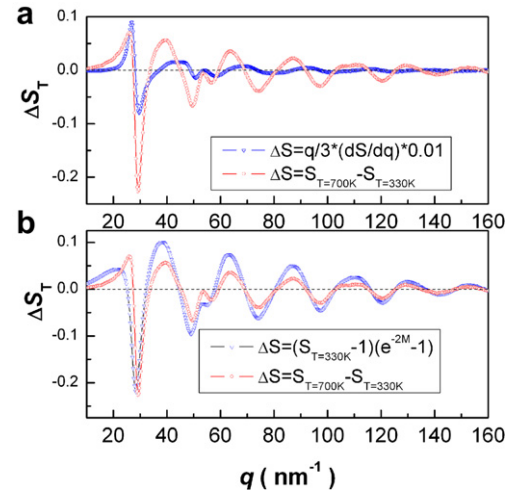


Fig. 6. Comparison of the measured change $\Delta S(q)_T$ with the calculations: a) for dilation of inter-atomic distances, b) for harmonic oscillations.

$$\Delta S(q)_T = -q^*(\delta S/\delta q)^*\epsilon = -q/3^*(\delta S/\delta q)^*(\Delta V/V) \quad (2)$$

with $\Delta V/V$ being the fractional volume expansion. Fig. 6a) compares the experimentally observed change of $\Delta S_{T=700 \text{ K}}$ with the calculation using Eq. (2) for 1.2% volume expansion. The obvious overall discrepancies indicate that the underlying assumption is not justified. Only the changes of $\Delta S_T(q)$ around the first maximum behave similar as can be seen in Fig. 6a), which is the reason that the shift in q_1 with temperature is approximately in accordance with the thermal expansion. The analysis of the shift of any other maxima of $S(q)$ with T would result in different values for the expansion coefficient, which is fundamentally different from the temperature dependence of the reflections of an isotropic crystalline material. Conversely, the thermal behaviour of the structure factor means that (reversible) changes of the relative atomic arrangement in the glass occur with temperature.

The influence of the thermal oscillations on the scattered X-ray intensities is described within the framework of the Debye theory [22]. The structure factor at a temperature T can be calculated from any temperature T_0 by the relation:

$$S_T(q) = 1 + (S_{T_0} - 1) \cdot \exp\left\{-2[W_T(q) - W_{T_0}(q)]\right\}, \quad W_T = \frac{3h^2q^2}{2m_a k_B \theta} \cdot \left(\frac{T}{\theta}\right)^2 \cdot \int_0^{\theta/T} \left(\frac{1}{2} + \frac{1}{e^z - 1}\right) z dz; \quad (3)$$

where $\exp(-2W_T)$ denotes the Debye–Waller factor, h is Planck's constant, k_B is Boltzmann's constant, m_a is atomic mass, and θ is Debye temperature.

For $T > \theta$ Eq. (3) can be approximated by:

$$S_T(q) = 1 + (S_{T_0} - 1) \cdot \exp\left\{-\frac{3h^2q^2}{m_a k_B \theta^2} [T - T_0]\right\}. \quad (4)$$

The thermal oscillation of the atoms is characterized by the mean-square displacement σ_D^2 and is given for $T \gg \theta$ by [22]: $\sigma_D^2 = (6h^2/m_a k_B \theta^2)T$.

From the temperature dependence of the height of the first maximum $S(q_1)$ one obtains $\theta = (240 \pm 12) \text{ K}$ for the $\text{Cu}_{65}\text{Zr}_{35}$ glass. Using Eq. (4) the change of the structure factor between $T = 330 \text{ K}$ and 700 K was calculated. Fig. 6b compares this calculation with the experimental observations. There is a qualitative agreement between the measurement and the calculations showing that the

Debye–Waller factor has an important influence and describes the reduction of the heights of the maxima. However, in detail differences occur especially in the first and the second maximum which are related to additional structural rearrangements of the atoms with temperature.

3.3. Analysis of real space data

From the structure factor $S(q)$ the reduced atomic pair correlation function $G(r) = 4\pi r(\rho(r) - \rho_0)$ was calculated by the Fourier transform of $S(q)$ between $0 \leq q \leq 220 \text{ nm}^{-1}$ [21]:

$$G(r) = 4\pi \cdot r \cdot (\rho - \rho_0) = \frac{2}{\pi} \cdot \int (S(q) - 1) \cdot q \cdot \sin(q \cdot r) \cdot dq, \quad (5)$$

where $\rho(r)$ is the atomic pair density distribution function and ρ_0 is the mean atomic density. For the $\text{Cu}_{65}\text{Zr}_{35}$ glass, a value of $\rho_0 = 63.7 \text{ nm}^{-3}$ is calculated from the mass density $\sigma_m = 7.75 \text{ g cm}^{-3}$. For multi-component glassy alloys, the atomic pair density function $\rho(r)$ represents a weighted sum of the element-specific partial atomic function $\rho_{ij}(r)$ which is also valid for the maxima of $G(r)$. In general it is not possible to extract unambiguously partial inter-atomic distances and coordination numbers from only one total atomic pair density distribution function. Here, we analyse the changes in $G(r)$ with temperature and compare them with the expectations assuming linear increase of inter-atomic distances and thermal harmonic oscillations, respectively. Fig. 7 compares the reduced atomic pair correlation functions $G(r)_T$ for different temperatures. With increasing temperature the shape of the first and the second maximum is altered and the positions of the maxima are shifted. The overall changes of $G(r)$ with temperature are displayed in Fig. 8 by the corresponding difference curves $\Delta G(r)_T = G(r)_T - G(r)_{T=330 \text{ K}}$. There is a monotonic increase of the amplitudes of $\Delta G(r)_T$ with temperature and, as found for the temperature change $\Delta S(q)_T/\Delta T$ of the structure factor, the relative change $\Delta G(r)_T/\Delta T$ does not depend on temperature T within the glassy state. The shape of the difference curves exhibits

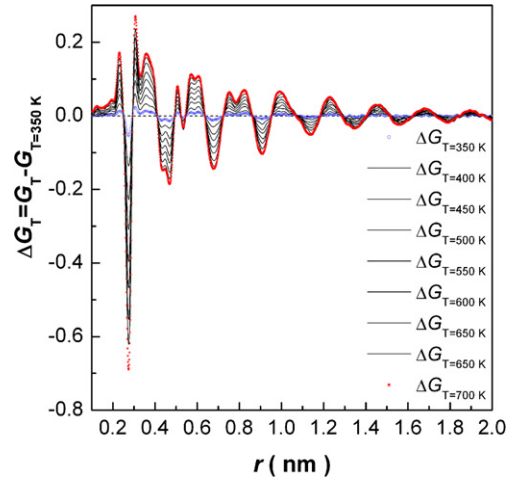


Fig. 8. Difference curves between $G(r)$ at room temperature and those at elevated temperatures.

a redistribution of the atoms especially within the first and second nearest neighbour shells. The two components of the first maximum exhibit a reversed dependence (inset in Fig. 7). The height of the first submaximum at $r_{11} = 0.276 \text{ nm}$ decreases with temperature and that of the second submaximum at $r_{12} = 0.316 \text{ nm}$ increases, respectively. For the second split maximum, the intensity ratio of the two submaxima is altered.

In the case of pure dilatation ($r_i(T) = r_i(T=0)(1 + \alpha T)$, $\Delta r_i = r_i \epsilon$) the change $\Delta G(r)_T$ should be proportional to the first derivative of the atomic pair correlation function $G(r)$ [23]:

$$\Delta G(r) = -r \cdot \frac{\partial G}{\partial r} \epsilon = -\frac{r}{3} \frac{\partial \Delta V}{\partial r} \quad (6)$$

The corresponding curves of $\Delta G(r)$ measured and calculated for $\epsilon = 0.004$ are compared in Fig. 9a. The differences are quite obvious for the first and second neighbourhood. However, at $r > 0.9 \text{ nm}$ the curves are almost identical. Fig. 9b compares the measured change of $G(r)$ with that of the expectation for increased thermal oscillation only. ΔG was calculated by the Fourier form of $\Delta S_T = (S_T = 330 \text{ K}(q) - 1) \cdot (e^{-2M} - 1)$. The underlying assumption of uncorrelated harmonic oscillations lead to a broadening of the distribution of inter-atomic distances or maxima of $G(r)$. The mean-square displacement σ_D^2 increases from $\sigma_D^2 = 0.00022 \text{ nm}^2$ for $T = 330 \text{ K}$ to $\sigma_D^2 = 0.00044 \text{ nm}^2$ for $T = 700 \text{ K}$. The comparison exhibits the occurrence of additional differences.

The positions r_i of the different maxima of $G(r)$ were calculated by Gaussian fits. A sum of two Gaussians was applied in order to extract the parameters of the two components of the first maximum (r_{11} and r_{12}) and those of the second maximum (r_{21} and r_{22}), respectively. The values r_{11} and r_{12} only approximately in accordance with the Cu–Zr and Zr–Zr nearest neighbour distances, because of the assumption of a Gaussian shape of the distribution function and also by neglecting the Cu–Cu contribution which can not be resolved in $G(r)$. Fig. 10 shows the relative change $\Delta r_i/r_i(T = 330 \text{ K})$ of the different maxima. The macroscopic expansion of the dilatometer measurement is also given for comparison. The positions of the maxima corresponding to the first maximum remain almost constant or even decrease with temperature. Also the second and third maxima deviate from the macroscopic thermal expansion. However, the shift of the maxima at $r > 0.9 \text{ nm}$ is in accordance with the macroscopically observed volume expansion. This means, changes in the short-range order occur with temperature, and the macroscopic volume expansion is reflected by the medium-range order. Fig. 11 shows the radial atomic pair

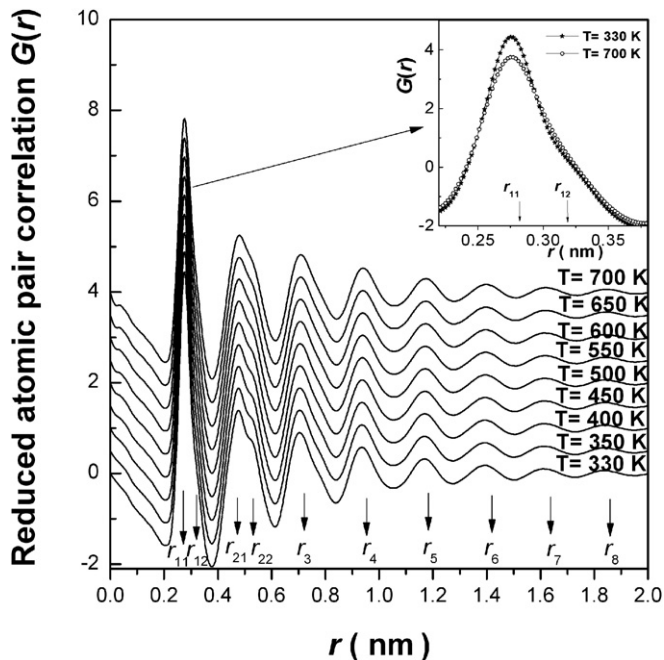


Fig. 7. Reduced atomic pair correlation function $G(r)$ of $\text{Cu}_{65}\text{Zr}_{35}$ glass at different temperatures.

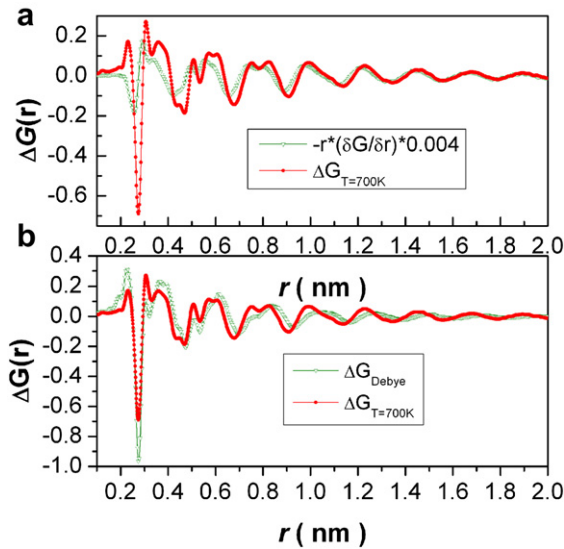


Fig. 9. Comparison of measured change $\Delta G(r)$ with calculations, a): for pure dilatation of inter-atomic distances, b): for thermal oscillations only.

density function $RDF = 4\pi r^2 \rho(r)$ at $T = 330$ K and 700 K, respectively. Also shown are the partial RDFs of $\text{Cu}_{65}\text{Zr}_{35}$ glass reported in [17]. As mentioned, the Cu-Cu contributions are not resolved and it is not possible to extract the three underlying partials reliably from the total RDF due to high correlation between the fit parameters and unknown profile function. An averaged nearest neighbour number N is obtained by integration over the total RDF in the interval between r_1 and r_2 :

$$N = \int_{r_1}^{r_2} 4\pi r^2 \cdot \rho(r). \quad (7)$$

The integration up to the first minimum ($r = 0.37$ nm) gives within the error limits identical coordination numbers $N^1 = 13.5$ for $T = 330$ K and $N^1 = 13.4$ for $T = 700$ K, respectively. Therefore, total nearest neighbour number of the $\text{Cu}_{65}\text{Zr}_{35}$ glass does not depend on temperature. However, beside of the broadening of the first neighbourhood by the thermal oscillations, the intensity ratio between the two components becomes additionally altered (Fig. 11).

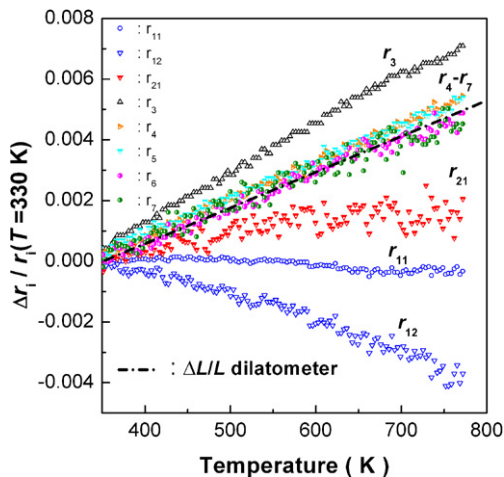


Fig. 10. Relative shift of interatomic distances r_i versus temperature (symbols) and that of macroscopic linear expansion (dashed line).

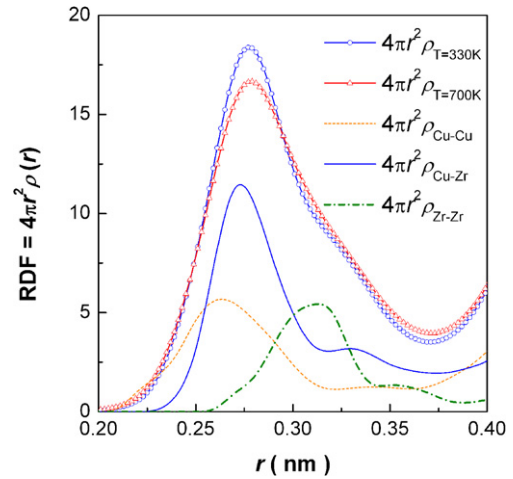


Fig. 11. Radial distribution function $4\pi r^2 \rho(r)$ of $\text{Cu}_{65}\text{Zr}_{35}$ glass at $T = 330$ K and 700 K. The underlying partial RDFs [17] are also given.

4. Discussion

One particular feature of the thermal behaviour of the $\text{Cu}_{65}\text{Zr}_{35}$ glass is that the nearest atomic neighbour distances do almost not alter with temperature, and therefore, do not reflect the macroscopic volume expansion. Such behaviour was also reported for other types of metallic glasses [24–26] and for metallic liquids [13], and also for element melts [27]. The reason for this behaviour is the occurrence of structural changes by (reversible) atomic rearrangements with temperature within the glassy and liquid state, which is different from that of crystalline alloys. In the glassy state each atom has an individual local environment which is accompanied by variation of the atomic level stresses [28]. Due to the disordered structure there is no possibility of a collective movement of all atoms in the same direction. Instead local atomic rearrangements occur depending on the corresponding atomic stress level.

Based on the concept of topological fluctuations and local atomic stresses of metallic glasses, an expression for the glass transition temperature T_g was derived recently, showing excellent agreement with experimental observations in metallic glasses [29]. This microscopic model assumes that for a critical volume strain of about 0.11, the atomic site becomes topologically unstable, and the local coordination may change. The local atomic level stresses define unstable (liquid-like) atomic sites and stable (solid-like) atomic sites. The density of the liquid-like atomic sites varies with temperature, and when it reaches the percolation limit the glass transition occurs [29]. The observed linear dependence of the (averaged) structural parameters of the $\text{Cu}_{65}\text{Zr}_{35}$ glass with temperature is in accordance with such a “two phase” system varying the fractions with temperature. The glass transition itself (not treated here) is however probably accompanied by further structural changes which are evident by the observation of different changes of the atomic pair correlation functions below and above T_g [20].

As discussed for the temperature dependence, it was shown in a recent publication that the glass transition can be also driven by applying stress [30]. Applied stress biases the stress distribution, and makes some atomic configurations unstable, or liquid-like. If the density of the liquid-like atoms exceeds the percolation limit the system flows like a liquid, thus mechanically inducing the glass-to-liquid transition. An intimate coupling of temperature and shear stress in inducing liquid-like flow in glasses was also concluded from the MD simulations [30]. On the experimental side, the

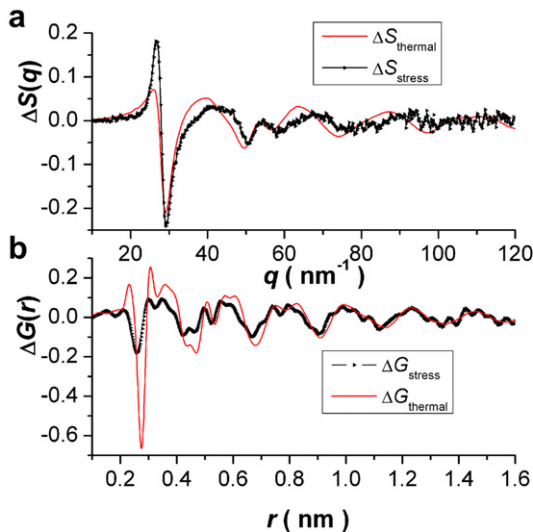


Fig. 12. Comparison of the influence of dilatation by temperature and by tensile stress a) on the structure factor and b) on the atomic pair correlation function. Changes of $\Delta S(q)$ and $\Delta G(r)$ of $\text{Cu}_{65}\text{Zr}_{35}$ glass correspond to an identical dilatation of 0.004 for all curves.

abundance of liquid-like sites in a BMG was reported by in situ X-ray diffraction experiments under tensile stress [31]. In this experiment a significant contribution of an elastic deformation was observed even though the applied stress was below the yield point. A fraction of an elastic sites of 24% was calculated, which coincides with the fraction of the liquid-like atoms which determine the glass transition [27,31].

In order to analyse to which extent thermal and mechanical strain are reflected in the short-range order of $\text{Cu}_{65}\text{Zr}_{35}$ glass, Fig. 12 compares a) the changes in the structure factor $S(q)$ and b) in atomic pair correlation functions $G(r)$ upon temperature with that upon tensile stress in the loading direction. The macroscopic length change $\Delta L/L_0 = 0.004$ is identical for both cases. The curves are in good agreement for the medium-range order at larger inter-atomic distances. However, the change of the short-range order of the glass exhibits differences between strain induced by temperature or by mechanical stress. One reason is probably that due to the uniaxial stress state the structure becomes an isotropic and the structural changes in the tensile direction are influenced by the compressive stress component.

5. Conclusions

The thermal behaviour of the short-range order of $\text{Cu}_{65}\text{Zr}_{35}$ metallic glass has been investigated by means of in situ high energy synchrotron X-ray diffraction. The analysis of the structure factor and the atomic pair correlation function as a function of temperature indicates reversible structural changes in addition to the effect of volume expansion and thermal oscillations. The structural

transformations are characterized by local atomic rearrangements as a consequence of the structural heterogeneity in the glass. The transformed fraction depends linearly on temperature within the glassy state. The experimental observations are in agreement with the finding of temperature dependent polyhedra statistics of the Cu-Zr glasses by MD simulation. The changes of the short-range order of the glass by thermal expansion are found to be different from those under elastic tensile strain.

Acknowledgements

The authors wish to express their thanks to Y. Zhang, I. Kaban, W. Dmoski and T. Egami for valuable discussions. Financial support of the Deutsche Forschungsgemeinschaft DFG (Ma 1531/10) is gratefully acknowledged.

References

- [1] Greer AL. Science 1995;267:1947.
- [2] Johnson WL. MRS Bull 1999;24:42.
- [3] Inoue A. Acta Mater 2000;48:279.
- [4] Yavari AR, Lewandowski JJ, Eckert J. MRS Bull 2007;32:635.
- [5] Inoue A, Takeuchi A. Acta Mater 2011;59:2243.
- [6] Xu D, Lohwongwatana B, Duan G, Johnson WL, Garland C. Acta Mater 2004;52:2621.
- [7] Wang D, Li Y, Sun BB, Sui ML, Lu K, Ma E. Appl Phys Lett 2004;84:4029.
- [8] Inoue A, Zhang W. Mater Trans 2004;45:584.
- [9] Wakeda M, Shibutani Y, Ogata S, Park J. Intermetallics 2007;15:139.
- [10] Cheng YQ, Cao AJ, Sheng HW, Ma E. Acta Mater 2008;56:5263.
- [11] Cheng YQ, Cao AJ, Ma E. Acta Mater 2009;57:3253.
- [12] Cheng YQ, Ma E. Prog Mater Sci 2011;56:379.
- [13] Mendelev MI, Kramer MJ, Ott RT, Soredelet DJ, Besser MF, Kreyssig, Goldman AI, et al. Phil Mag 2010;90:3795.
- [14] Almyras GA, Lekka CE, Mattern N, Evangelakis GA. Scripta Mater 2010;62:33.
- [15] Mattern N, Schops A, Kuhn U, Acker J, Khvostikova O, Eckert J. Non-Cryst Solids 2008;354:1054.
- [16] Wang XD, Yin S, Cao QP, Jiang JZ, Franz H, Jin ZH. Appl Phys Lett 2008;92:011902.
- [17] Mattern N, J  v  ri P, Kaban I, Gruner S, Elsner A, Kokotin V, et al. J Alloys Comp 2009;485:163.
- [18] Almyras GA, Papageorgiou DG, Lekka CE, Mattern N, Eckert J, Evangelakis GA. Intermetallics 2011;19:657.
- [19] Wessels V, Gangopadhyay AK, SahuKK Hyers RW, Caneparri SM, Rogers JR, Kramer MI, et al. Phys Rev B 2011;83:094116.
- [20] Hammersley AP, Svensson SO, Hanfland M, Fitch AN, Haeusermann D. High Press Res 1996;14:235, <http://www.esrf.eu/computing/scientific/FIT2D/>.
- [21] Wagner CNJ. In: Beer SZ, editor. Liquid metals, chemistry and physics. New York: Marcel Dekker Inc.; 1972. p. 257.
- [22] Sinha S, Srivastava PL, Singh RN. J Phys Condens Matter 1989;1:1695.
- [23] Suzuki Y, Haimovich J, Egami T. Phys Rev B 1987;35:2162.
- [24] Mattern N, Hermann H, Roth S, Sakowski J, Macht HP, Jovari P, et al. Appl Phys Lett 2003;82:2589.
- [25] Bednarcik J, Michalik S, Sikorski M, Curfs C, Wang XD, Jiang JZ, et al. Phys Condens Matter 2011;23:254204.
- [26] Georgarakis K, Louzguine-Luzgin DV, Antonowicz J, Vaughan G, Yavari AR, Egami T, et al. Acta Mater 2011;59:708.
- [27] Schenk T, Holland-Moritz D, Simonet V, Bellissent R, Herlach DM. Phys Rev Lett 2002;89:075507.
- [28] Egami T. Prog Mater Sci 2011;56:637.
- [29] Egami T, Poon SJ, Zhang Z, Keppens V. Phys Rev B 2007;76:024203.
- [30] Guan P, Chen M, Egami T. Phys Rev Lett 2010;104:205701.
- [31] Dmowski W, Iwashita T, Chuang CP, Almer J, Egami T. Phys Rev Lett 2010;105:205502.